

Comparative analysis of FSO links with various modulation formats under controlled turbulence

GIREESH G. SONI^{1,*}, ABHISHEK TRIPATHI^{2,*}, MANASWI SHROTI¹, KUSHAGRA AGARWAL¹, RAMCHANDRA GURJAR¹

¹Shri G S Institute of Technology and Science, Indore, MP, India

²Kalasalangam Academy of Research and Education, Srivilliputhur, TN, India

This work investigates the propagation of modulated optical signals under controlled turbulence conditions. Atmospheric channel are emulated in a laboratory testbed, where turbulence is characterized by varying the wind pressure and temperature inside the chamber. The observed turbulence index structure parameter (C_n^2) lies in the range of 10^{-15} to 10^{-13} , which indicates the Gamma-Gamma ($\Gamma\Gamma$) channel model. It is observed that the turbulence strength is increased inside the chamber as temperature increases, and increase in the wind pressure leads to variation in C_n^2 values. The system performance is compared by employing various modulation schemes namely amplitude shift keying (ASK), frequency shift keying (FSK), and binary phase shift keying (BPSK) under turbulence. A 10 meter single input single output (SISO) optical link is used to observe the performance metrics of signal-to-noise ratio (SNR), bit error rate (BER), and outage probability. It is found that the system indicates the better performance for BPSK modulation. The higher SNR values range (from 7.26 dB to 8.82 dB) is obtained for BPSK, followed by the performance of FSK and ASK. A minimum average outage is observed for BPSK which is comparable to ASK, however, the latter requires a slightly higher SNR to achieve the same outage probability.

(Received March 20, 2023; accepted October 9, 2023)

Keywords: Free Space Optics (FSO), Atmospheric Turbulence, Modulations formats

1. Introduction

Free Space Optics (FSO) is a line-of-sight (LoS) technology where light is used as a carrier to transfer information over distances extending from a few meters to hundreds of meters. In this technology, the message signal is modulated on an optical carrier and is then allowed to propagate through the free space atmospheric channel, rather than guided channels. Though physical medium such as fiber cables offer huge bandwidth and are power efficient but deploying them is a time-consuming and the last-mile bottleneck [1,2]. Alternatively, though RF communication possesses high beam divergence providing network access to various users, but has low power, low spectral efficiency, and supports limited data rates. FSO has emerged as an alternative to their counterpart and has been researched as a complementary technology for establishing high data rate links over short distances, thus facilitating the access networks in the existing backbone networks. It has multiple advantages and it is a viable technique to fulfill the bandwidth requirement of various end users, ease of deployment, low power consumption, high security, and considerable reduction in cost and time [3,4]. Some hybrid architectures have been reported for successful multigigabit transmission over FSO link [5-7]. The development of optoelectronic devices led to the expansion of FSO links over the past decade and find suitability in applications of last-mile access, enterprise connectivity, fiber backup, bridging WAN access, and military access [8].

Some challenge to the traverse of optical signal in outdoor FSO link is the induced noise in information signal due to obstacles such as trees, buildings, building sway and birds [9]. The major impairments comes due to prevailing environmental conditions such as scintillation, rain, dust, snow, fog etc. Wind pressure and temperature cause fluctuations in air density, resulting in the formation of eddies, which are local unstable air masses with varying refractive indices. These eddies act as prisms of variable sizes and hence result in the fluctuation of the phase and intensity of the received signal [10].

One of the main parameters in describing the turbulence is the R.I. structure parameter (C_n^2) indicating the change in R.I. of air. Hufnagel-Valley model in Eq. (1) is more suitable to describe C_n^2 , where its value varies with altitude [11,12]:

$$C_n^2 = 0.00594 \left(\frac{v}{27}\right)^2 \left(\frac{h_v}{10^5}\right)^{10} m^{-\frac{2}{3}} \exp\left(-\frac{h_v}{1000}\right) + 2.7 \times 10^{-16} m^{-\frac{2}{3}} \exp\left(-\frac{h_v}{1500}\right) + 1.7 \times 10^{-14} m^{-\frac{2}{3}} \exp\left(-\frac{h_v}{100}\right) \quad (1)$$

where, h_v = Altitude in metre, v = Wind speed in m/s .

However, the values of C_n^2 can be calculated by measuring pressure of wind (P) = $0.00613 \times v^2$ [10], and

temperature structure parameter ($C_n^2 = \langle \delta T^2 \rangle r^{-1/3}$ using Eq. (2) [14]:

$$C_n^2 = \left(86 \times 10^{-6} \times \frac{P}{T^2} \right)^2 C_T^2 \quad (2)$$

where, P in millibar; Average temperature (T) in Kelvin, and δT is the temperature difference between two points separated by the propagation distance (r).

Many methods have been tried to reduce the distortions in the channel and retrieve as error-free information as possible including diversity techniques, aperture averaging etc. [15,16]. The choice of modulation formats also plays a role in increasing the quality of the received signal [17]. Multiple pieces of research have been conducted experimenting with modulation techniques, channel models, and reception techniques to increase the link performance and to understand which methods work best with the selected set of environmental conditions [18-20]. Comparison of various modulation formats, various diversity, and combining techniques for different turbulence conditions and channel models is still being explored.

In this work, turbulence strength is the varied and the values of C_n^2 is calculated. We attempt to comprehend the effect of turbulence on modulated signals in this paper. The signal quality is estimated by calculating the SNR, BER and outage probability for the modulation formats of ASK, FSK, and BPSK. Section 2 describes the experimental system and methodology. Section 3 discusses the obtained communication metrics in turbulence variation as function wind flow and temperature. Section 4 concludes the work.

2. System description

The experimental setup in Fig. 1 is primarily consisted of three sections: Transmitter, channel, and receiver section. A subcarrier-modulated signal generated using an arbitrary function generator, AFG31002, is connected to a laser driver, and a laser diode (LD) that acts as a carrier, eventually generates a modulated signal. The LD has an average power of 3 mW and 650 nm wavelength and is placed on an XYZ translational stage to ease movement and maintain LOS. This wavelength is selected because it comes under one of the communication windows and has the easy availability of the components and is cost-effective. The channel is a closed transparent chamber made of acrylic sheets and has dimensions of $5 \times 0.5 \times 0.5 \text{ m}^3$. The turbulence effect is calculated by varying the atmospheric conditions which are imitated in the chamber as closely as possible to match the outdoor environmental conditions using controlled fans and heating coils. Eight fans are placed along the length of the chamber and the direction of the air is transverse to the signal direction and hotplate are fixed on the floor to provide temperature variation. Four thermometers and anemometers are placed for measuring the temperature and wind speed, respectively. Holes are drilled on top plane and the plane opposite fans to maintain air circulation for trying to replicate the real time scintillation.

The signal is detected using a silicon PIN photodiode and responsivity of 0.45 A/W followed by an oscilloscope, and data accumulation system to analyze the performance. Thorlabs S121C Standard Photodiode with power Sensor and Thorlabs PM400 Laser Power Meter are used for the detection of the signal.

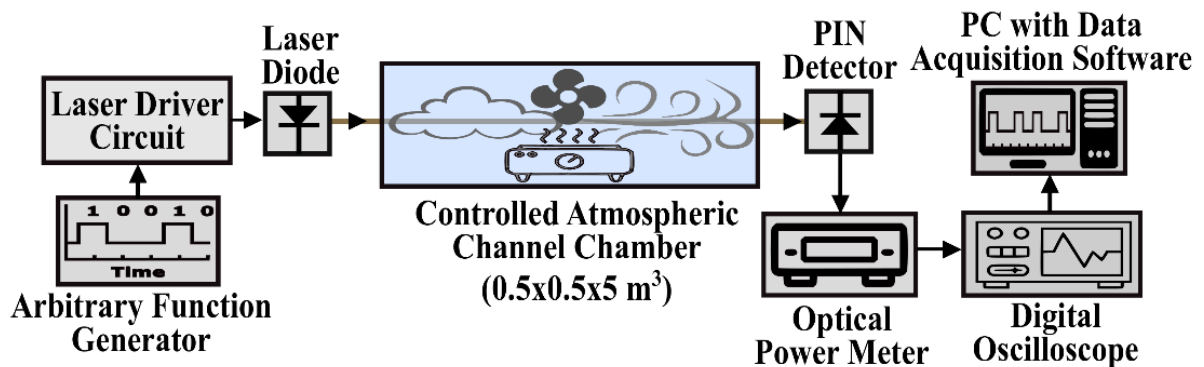


Fig. 1. Schematic of the experimental testbed for FSO link under controlled atmospheric condition

3. Results and discussions

The structure parameter C_n^2 values are calculated for different wind speeds, 1, 1.5, 2, and 2.5 m s^{-1} . It is found in the range of $2.69 \times 10^{-15} \text{ m}^{-2/3}$ to $2.32 \times 10^{-13} \text{ m}^{-2/3}$ indicating the turbulence conditions to

be moderately strong. Fig. 2 shows variations in C_n^2 with temperature for four different wind speeds. It is observed that as temperature increases, the value of C_n^2 increases which imply an increase in the turbulence created inside the chamber.

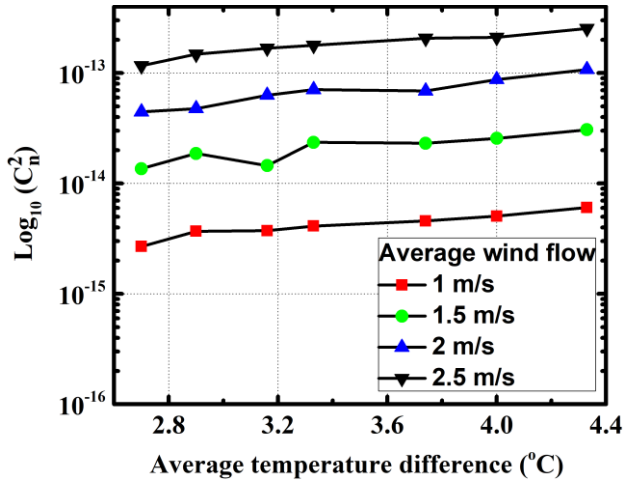


Fig. 2. Plot of C_n^2 as a function of average temperature difference under the effect of different wind speeds (color online)

Variation in average C_n^2 values with wind speed are shown in the Fig. 3 below. The C_n^2 values are measured when the temperature in the chamber was close to saturation, i.e., around 42 °C. The variation in C_n^2 values over multiple calculations are shown through error bars and it is observed that as the wind pressure increases, the variation in the C_n^2 values increases.

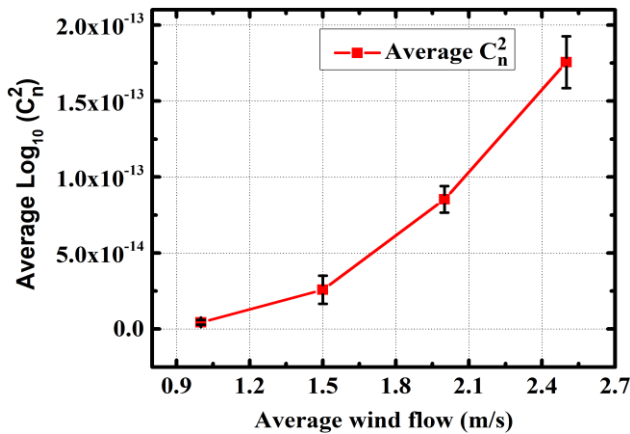


Fig. 3. The graph for C_n^2 versus average wind speeds

Fig. 4 shows the variation in BER vs SNR for ASK, FSK, and BPSK modulation formats and it is observed that the BER reduces as SNR is increased. The SNR values range from 7.26 dB to 8.82 dB for BPSK, from 4.83 dB to 12.99 dB for FSK, and 1.24 dB to 13.73 for ASK. The BER values, on the other hand, range from 0.0003 to 0.0025 for BPSK, from 0.0001 to 0.1129 for FSK, and 0.0307 to 0.419 for ASK.

It can also be observed that the range of SNR values for ASK is largest followed by FSK and BPSK. The variation in the SNR comes due to their waveforms. In the case of a BPSK-modulated signal, the amplitude of the irradiance values remains the same at the detector when bit

'0' and bit '1' are transmitted whereas, in the case of FSK, the irradiance varies when bit 0 and bit 1 are transmitted. In the case of ASK, the irradiance varies largely for bit '1' and bit '0' as the signal has zero amplitude when bit '0' is transmitted.

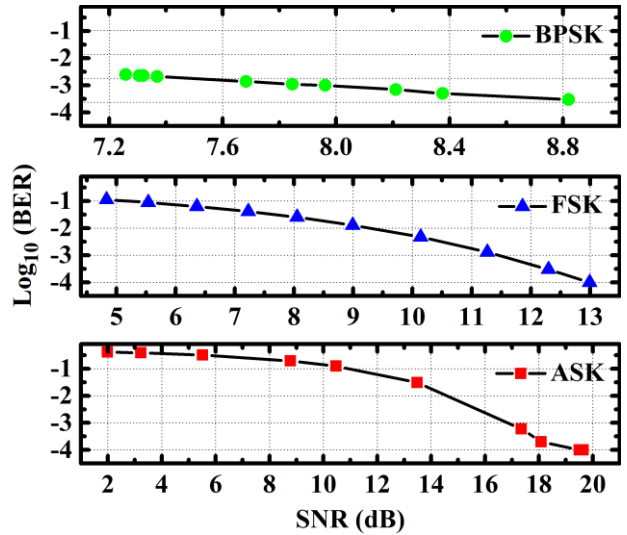


Fig. 4. The BER measurement versus SNR for the modulation formats of ASK, BPSK and FSK (color online)

FSK and ASK provide high SNR values as compared to BPSK but these values become equally small when bit 0 is transmitted. On the other hand, SNR values for BPSK have a small range. For this reason, BPSK is preferable. The figure below shows the outage probability against the SNR values for BPSK, FSK, and ASK modulation formats. The plot in Fig. 5 shows that BPSK has a maximum outage probability of 0.38, whereas, for FSK and ASK, the maximum outage is 0.52 and 0.99, respectively. The outage is measured at the threshold of 7.47 dB. Due to the smaller range of SNR values in the case of BPSK, the threshold for SNR is lesser as compared to FSK and ASK where the SNR range is much more.

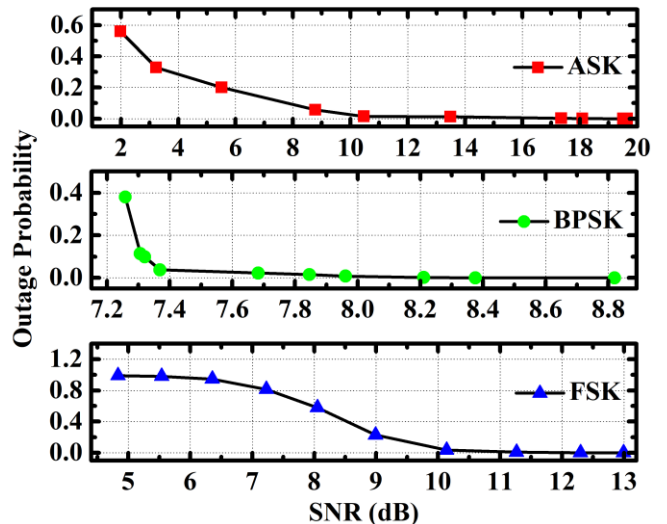


Fig. 5. Variation of outage probability as a function of SNR for selecting three separate modulation formats (color online)

4. Conclusion

For terrestrial FSO links, scintillation (turbulence) is a major factor in beam wandering, wavefront fluctuations, and phase distortion of optical signals. An experimental setup to investigate turbulence-induced impairments on the optically modulated signals propagating in free space is developed and characterized in which varying turbulence conditions are imitated. It is calibrated for varying magnitudes of refractive index structure parameters by regulating the wind flow and the temperature inside the channel. The observed turbulence parameter (C_n^2) lies in the range of $2.69 \times 10^{-15} m^{-2/3}$ to $2.32 \times 10^{-13} m^{-2/3}$, which indicates the gamma-gamma channel model. A comparison of various modulation schemes employed namely ASK, FSK, and BPSK in presence of controlled turbulence is carried out. A 10-meter SISO optical link is used to observe the BER, SNR, and probability of outage. It is found that for a specific BER, the SNR requirement is minimum in the case of BPSK followed by FSK and ASK. The minimum average outage is observed for BPSK which is comparable to ASK, however, the latter requires a slightly higher SNR to achieve the same outage probability. Moreover, ASK provides higher SNR as compared to FSK followed by BPSK but the SNR values reduce equally. Even though BPSK provides a smaller SNR range, the fluctuations in SNR are less making it preferable to ASK and FSK.

Acknowledgement

This work is supported by CRS research Grant No.1-5763970771 received from NPIU, MHRD under TEQIP-III to Dr. Gireesh G. Soni, Shri G. S. Institute of Technology and Science, Indore, India. We also thank lab staff of Optical Communication laboratory, Shri G. S. Institute of Technology and Science for the support.

References

- [1] A. Malik, P. Singh, International Journal of Optics **2015**, 1 (2015).
- [2] Z. Ghassemlooy, W. Popoola, S. Rajbhandari, Optical Wireless Communications: System and Channel Modelling with MATLAB®, CRC Press 2017.
- [3] D. J. T. Heatley, D. R. Wisely, I. Neild, P. Cochrane, IEEE Communications Magazine **36**, 72 (1998).
- [4] S. Bloom, E. Korevaar, J. Schuster, H. Willebrand, Journal of Optical Networks **2**, 178 (2003).
- [5] S. Magidi, A. Jabeena, Wireless Personal Communications **119**(4), 2951 (2021).
- [6] M. Singh, J. Kriz, M. M. Kamruzzaman, V. Dhasarathan, A. Sharma, S. A. Abd El-Mottaleb, Frontiers in Physics **10**, 934848 (2022).
- [7] S. Chaudhary, L. Wuttisittikulij, J. Nebhen, A. Sharma, D. Z. Rodriguez, S. Kumar, PlosOne **17**(3), 0265044 (2022).
- [8] X. Zhu, J. M. Khan, IEEE Transaction on Comm. **50**(8), 1293 (2022).
- [9] J. Jeyarani, D. Sriramkumar, B. E. Caroline, J. Optoelectron. Adv. M. **20**(9-10), 506 (2018).
- [10] G. G. Soni, A. Tripathi, A. Mandloi, S. Gupta, Optical and Quantum Electronics **51**, 172 (2019).
- [11] W. O. Popoola, Z. Ghassemlooy, C. G. Lee, A. C. Boucouvalas, Optics & Laser Technology **42**(4), 682 (2010).
- [12] A. K. Majumdar, J. C. Ricklin, Free-Space Laser Communications: Principles and Advances, 2008 edition, NY: Springer Science & Business Media, 2007.
- [13] M. Chaudhary, B. Vyas, M. Katoch, P. Negi, T. Miroshnikova, Materials Today: Proceedings **69**, 524 (2022).
- [14] Z. Ghassemlooy, H. Le Minh, S. Rajbhandari, J. Perez, M. Ijaz, Journal of Lightwave Technology **30**(13), 2188 (2012).
- [15] A. Viswanath, V. K. Jain, S. Kar, Optical and Quantum Electronics **48**, 435 (2016).
- [16] H. Kaushal, V. Kumar, A. Dutta, H. Aennam, V. K. Jain, S. Kar, J. Joseph, IEEE Photonics Technology Letters **23**(22), 1691 (2011).
- [17] N. Bhan, S. Kaur, N. Nair, J. Optoelectron. Adv. M. **24**(5-6), 221 (2022).
- [18] M. A. Esmail, Optics Communications **486**, 126776 (2021).
- [19] A. Tripathi, S. Gupta, A. Mandloi, G. G. Soni, Journal of Modern Optics **69**(8), 419 (2021).
- [20] F. Xu, A. Khalighi, P. Caussé, S. Bourennane, Optics Express **17**(2), 872 (2009).

*Corresponding author: tripathi.abhishek.5@gmail.com
gireeshsoni@gmail.com